Supplementary Information

Medium ion-association electrolyte enabled fast and stable K-storage for organic ferrocene anode

Jing Zheng[1,*], Qun Li[1], Hao Wang[1], Jijian Xu[2,*], Xiaokang Chu[1], Ran Chen[1], Haobo Xia[3], Jianying Long[1], Meng Lei[1], Mengtao Ma[1], Zixia Lin[4], Qingxue Lai[3,*]

[1]*Department of Chemistry and Materials Science, College of Science, Nanjing Forestry University, Nanjing 210037, P. R. China*

[2]*Department of Chemistry, City University of Hong Kong, Hong Kong 999077, China*

[3]*Jiangsu Key Laboratory of Electrochemical Energy Storage Technologies, College of Materials Science and Technology, Nanjing University of Aeronautics and Astronautics, Nanjing 210016, P. R. China*

[4]*Testing Center, Yangzhou University, Yangzhou 225009, P. R. China*

*Corresponding Author: jzheng62@njfu.edu.cn;
jijianxu@cityu.edu.hk;
qx_lai@nuaa.edu.cn;

Supplementary Figures

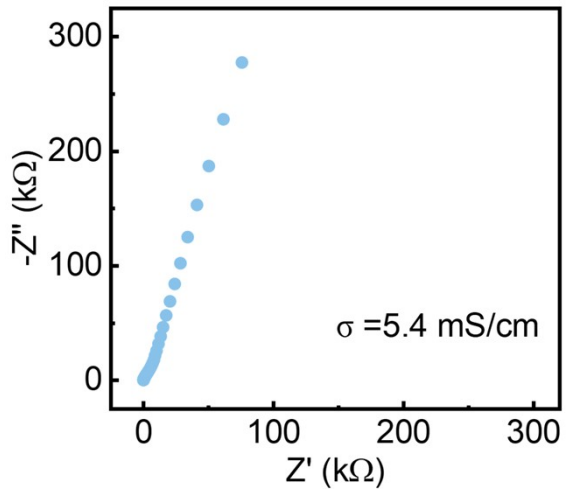

Figure S1. EIS test and ionic conductivity of 3M KFSI/DMC.

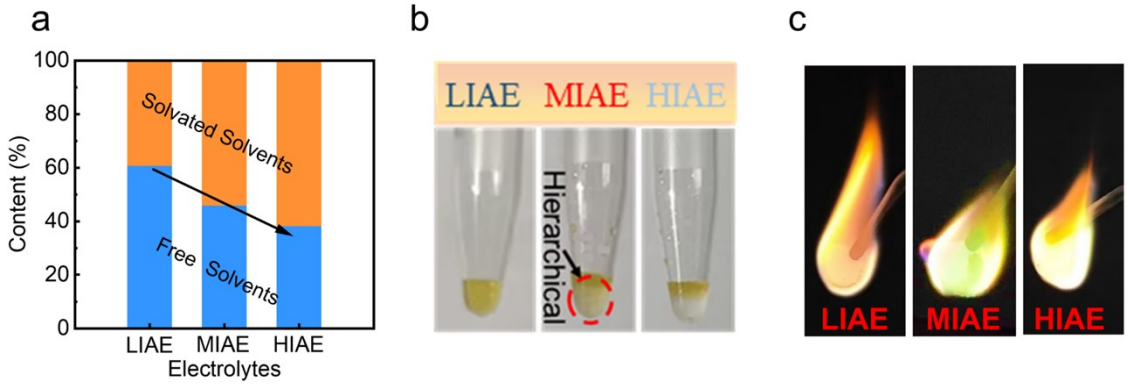

Figure S2. Calculated contents a) of solvated structure from Raman spectra; solubility test b) of Fc in electrolytes; digital photo of maximum flame height c) of combustion test.

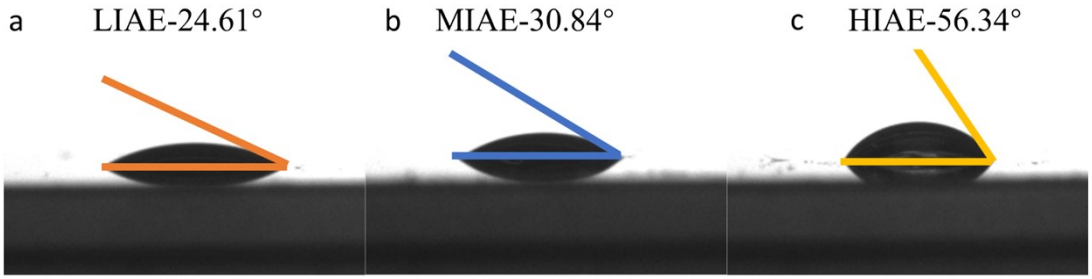

Figure S3. Wettability test of three electrolytes: a) LIAE, b) MIAE, c) HIAE.

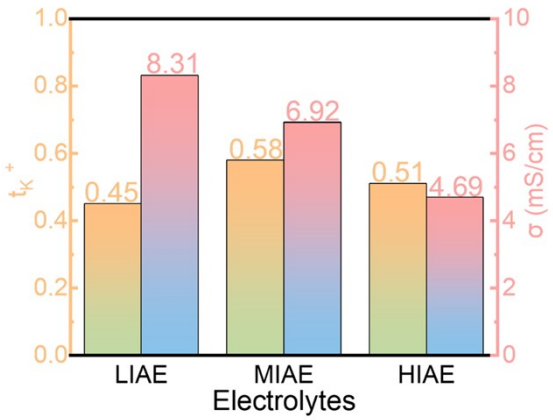

Figure S4. Transference number and ionic conductivity of LIAE, MIAE and HIAE

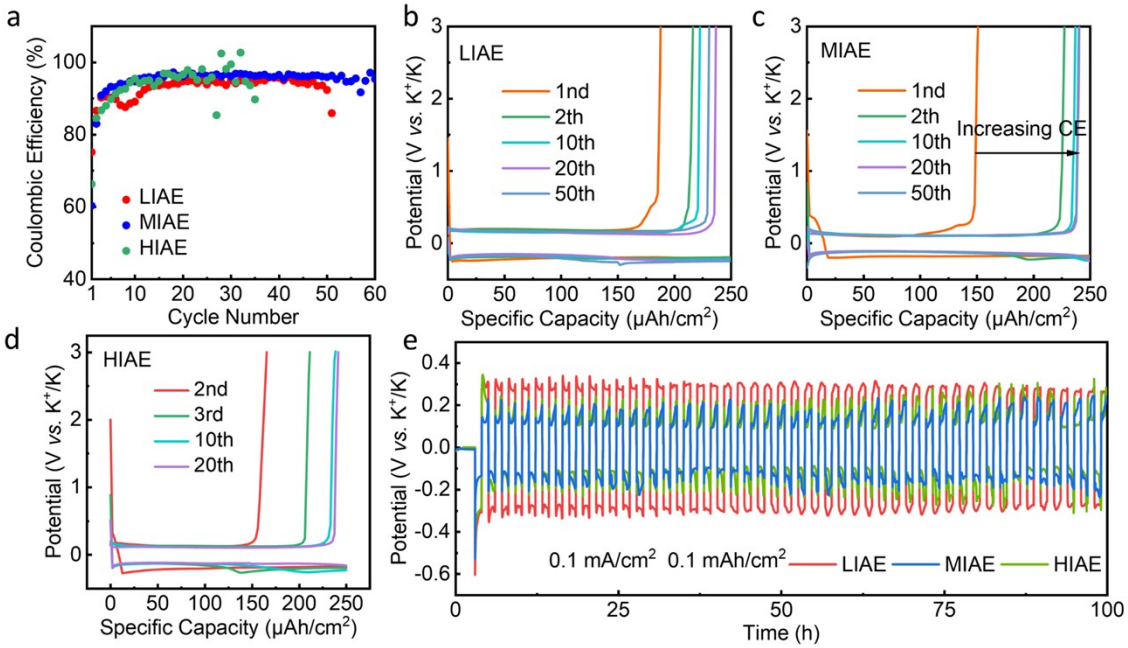

Figure S5. Compatibility test for K-metal: a) coulombic efficiency of K||Cu cells; voltage-capacity curves for K plating/stripping in b) LIAE, c) MIAE, d) HIAE; e) cycling performance of K||K symmetric cells assembled with different electrolytes.

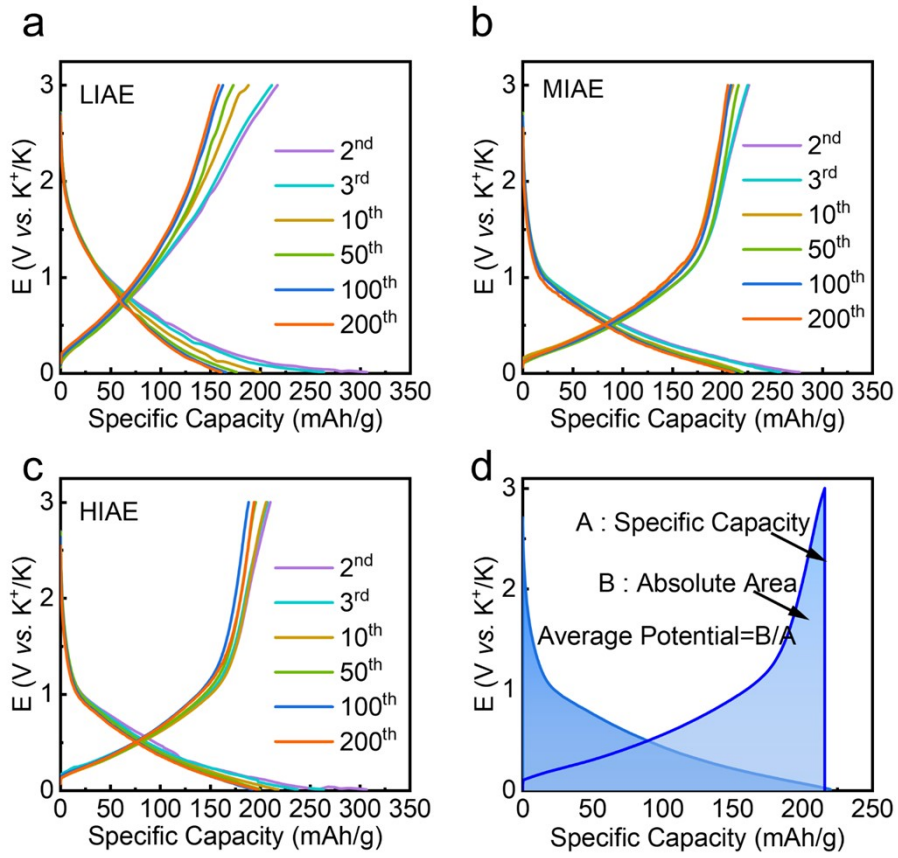

Figure S6. GDC of Fc at 50 mA/g in a) LIAE, b) MIAE and c) HIAE; Schematic diagram d) for calculating average potential.

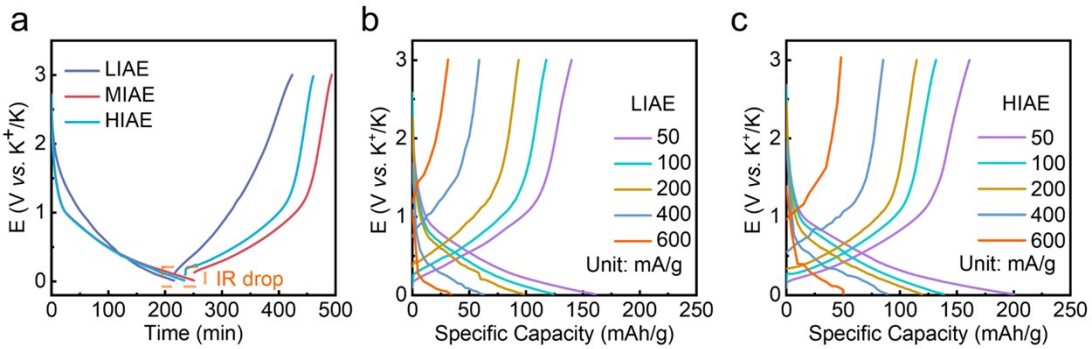

Figure S7. IR drop a) from GDC curves in different ion-association electrolytes at 50 mA/g; GDC curves at various rates in b) LIAE and c) HIAE.

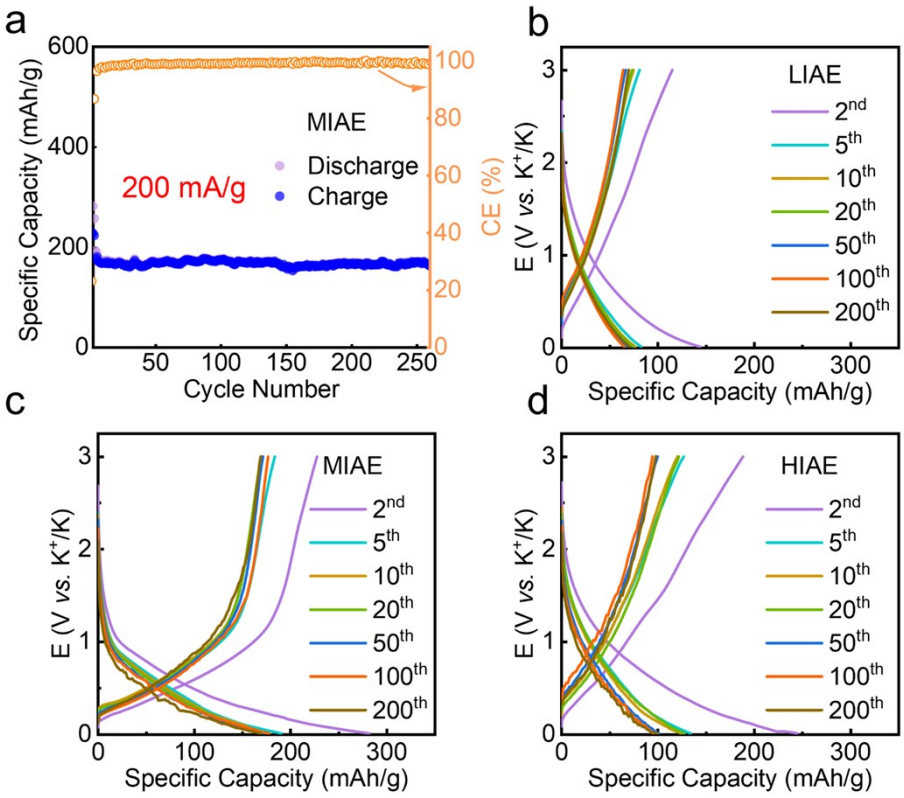

Figure S8. Long cycle performance of Fc a) at 200 mA/g in MIAE; GDC of Fc at 200 mA/g in b) LIAE, c) MIAE, d) HIAE.

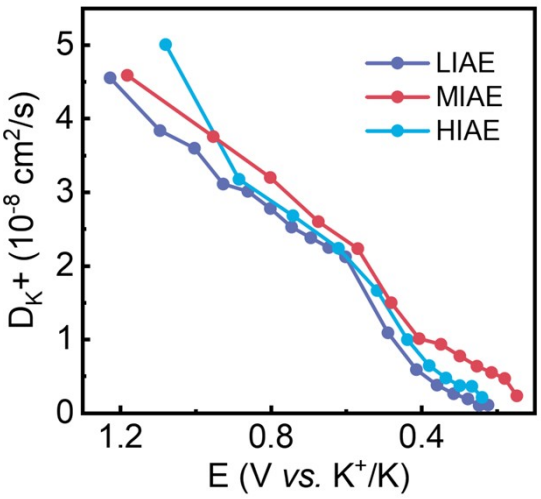

Figure S9. D_{K^+} during the potassiation process.

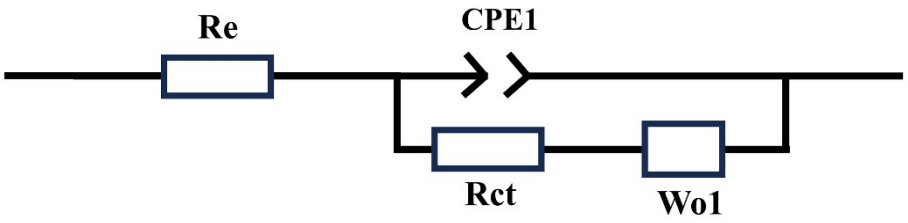

Figure S10. Corresponding fitting circuit of cells.

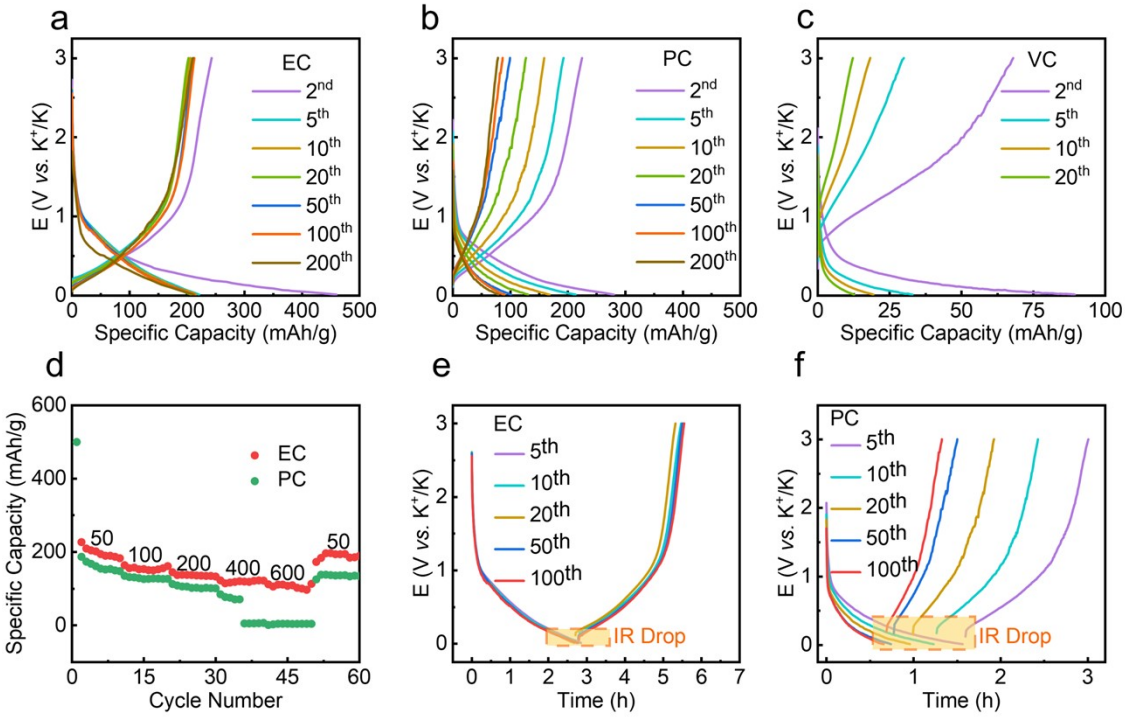

Figure S11. GDC of Fc at 100 mA/g in a) EC-based, b) PC-based and c) VC-based MIAE; rate performance d) in these electrolytes; calculated IR drop comparison from GDC curves in e) EC-based and f) PC-based MIAE.

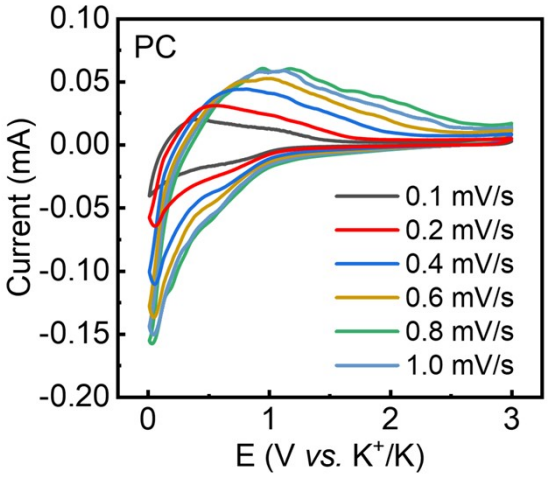

Figure S12. CV curves of Fc in PC-based MIAE at scan rates across 0.1-1.0 mV/s.

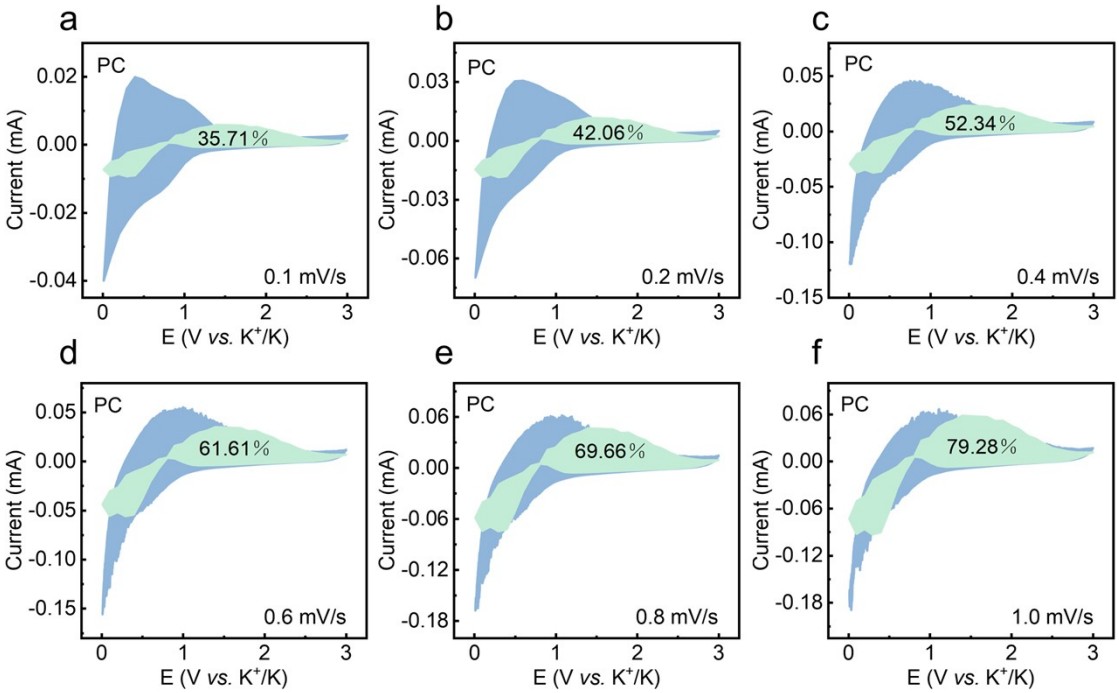

Figure S13. Surface capacitance contributions of Fc anode in PC-based MIAE at different scan rates: a) 0.1 mV/s, b) 0.2 mV/s, c) 0.4 mV/s, d) 0.6 mV/s, e) 0.8 mV/s, f) 1.0 mV/s.

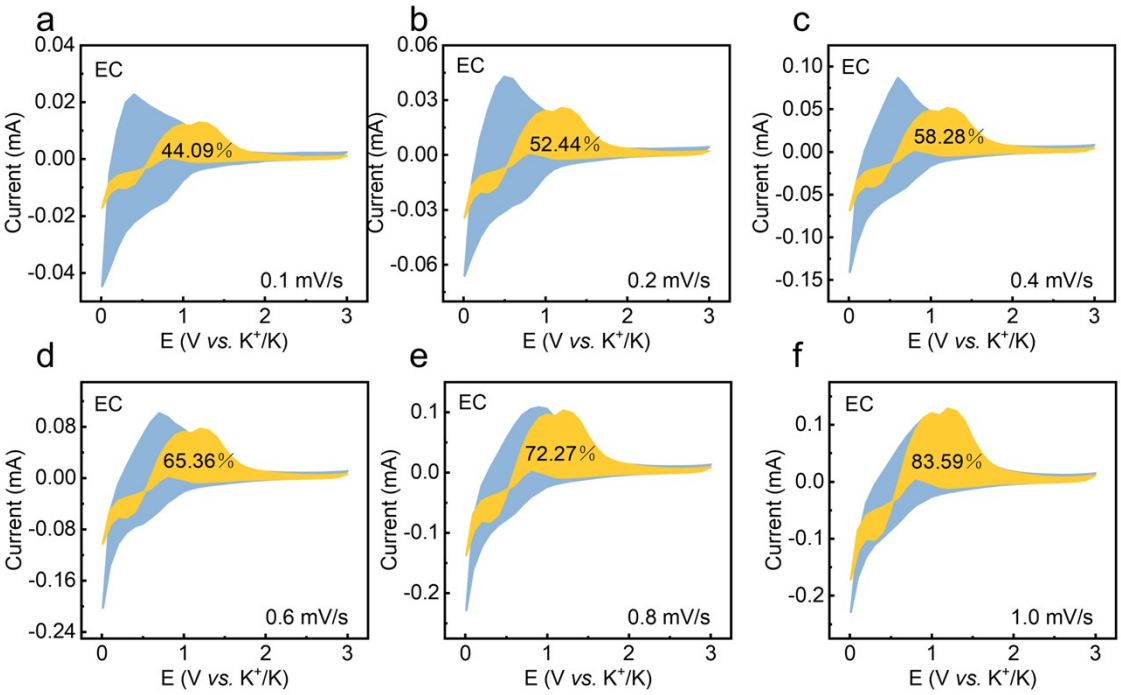

Figure S14. Surface capacitance contributions of Fc anode in EC-based MIAE at different scan rates: a) 0.1 mV/s, b) 0.2 mV/s, c) 0.4 mV/s, d) 0.6 mV/s, e) 0.8 mV/s, f) 1.0 mV/s.

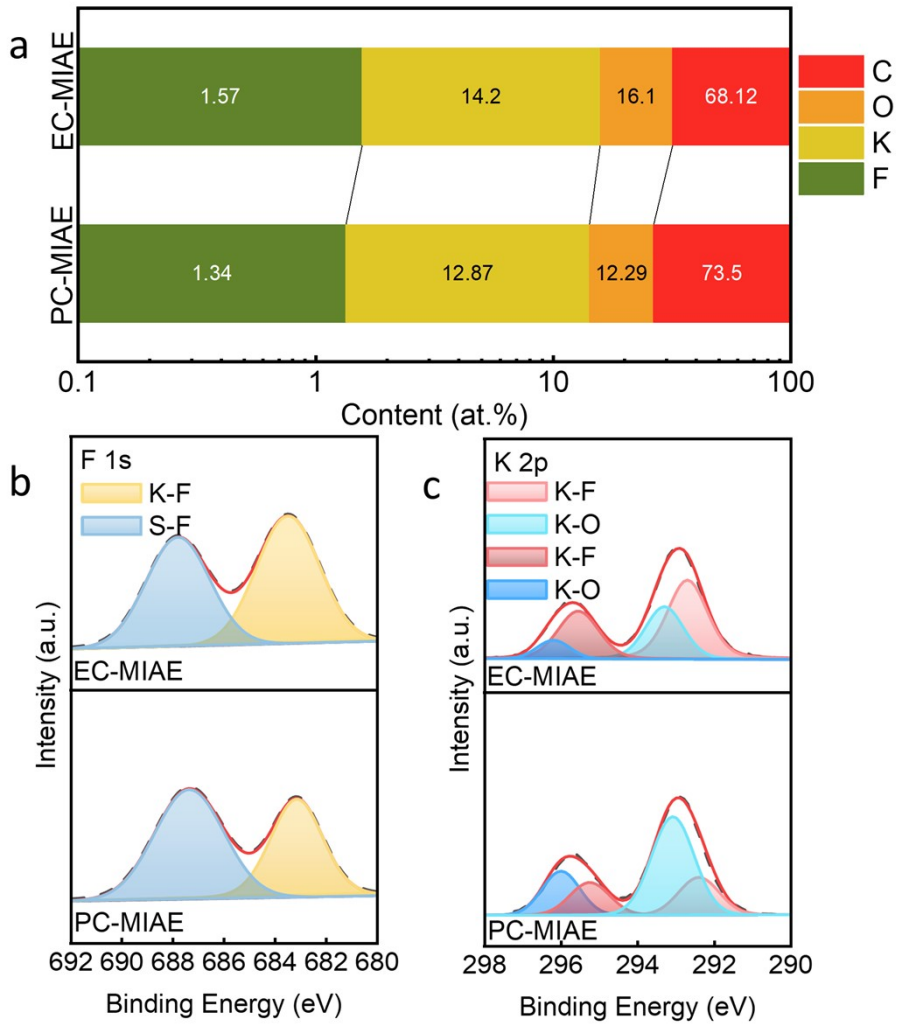

Figure S15. SEI compositional analysis: a) elemental distribution on the surface of Fc after cycling; XPS spectra of b) F 1s, c) K 2p for Fc after cycling in the EC-based MIAE and PC-based MIAE.

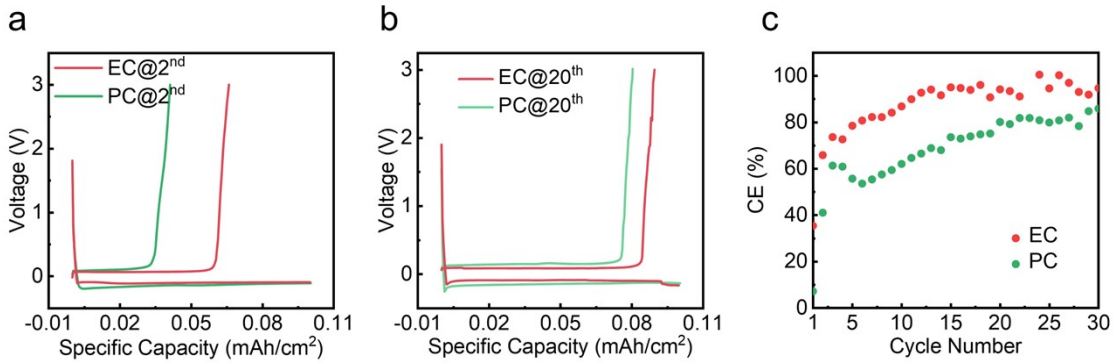

Figure S16. Electrochemical performance of K||Cu cells: voltage profiles during K plating/stripping at a) 2nd and b) 20th cycles, and c) long-term cycling stability in different electrolytes.

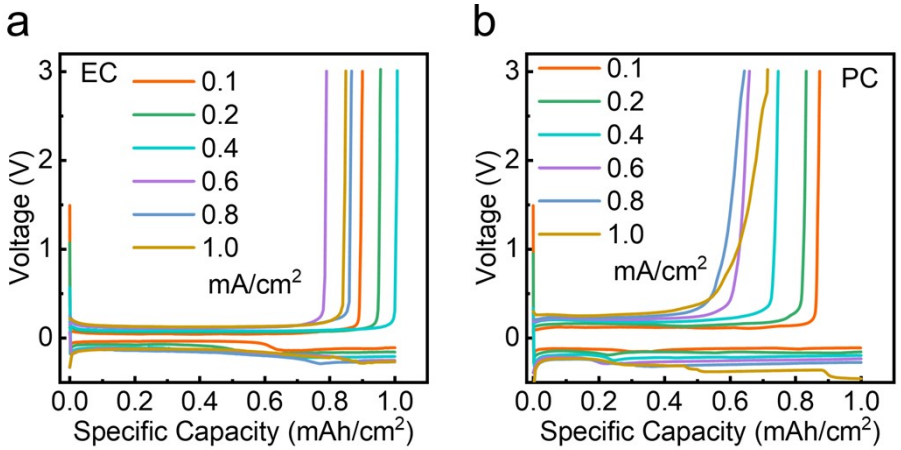

Figure S17. Voltage profiles of K||Cu cell a) with EC-based MIAE and b) with PC-based MIAE at different current densities.

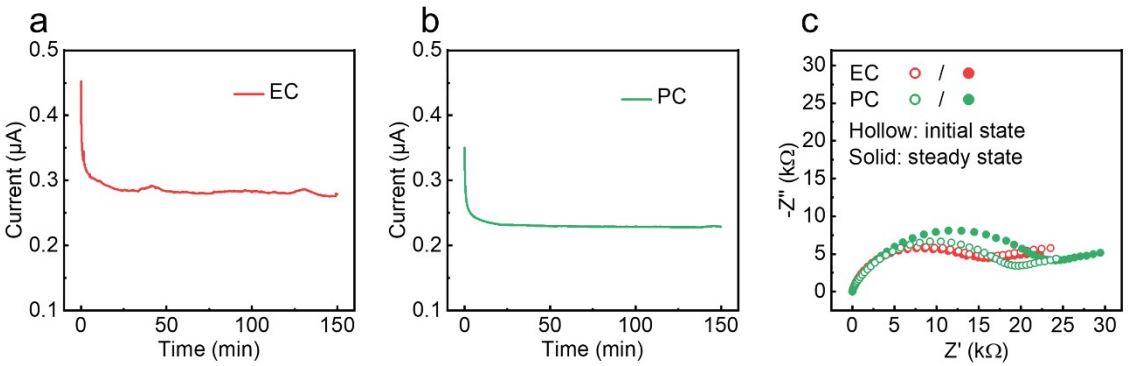

Figure S18. Chronoamperometry curves in a) EC-based and b) PC-based MIAE; c) EIS tests before and after polarization.

Table S1. Comparison of specific capacities with previously reported organic K-storage anodes.

Organic Anode	Structural Formula	Current Density (mA/g)	Specific Capacity (mAh/g)	Electrolyte	References
Fc	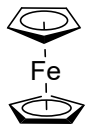	50 200	209.1 171.9	3M KFSI/EC+DMC (1:1, by vol)	This work
HAT-COOK	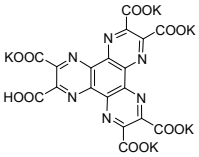	50	207	1M KFSI/EC+DEC (1:1, by vol)	S1
K_2PC	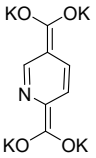	50	190	1M KFSI/EC+DMC (1:1, by vol)	S2
CTF-1		50	176	0.8M KPF_6/EC+DEC (1:1, by vol)	S3
K_2BPDC	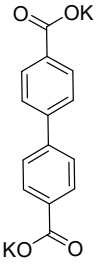	50	170	1M KFSI/EC+DMC (1:1, by vol)	S4
$[C_7H_3KNO_4]_n$		50	168	1M KFSI/EC+DMC (1:1, by vol)	S5
ADAPTS	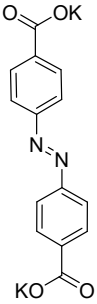	50	138	1 M KFSI/EC +DEC (1:1, by vol)	S6

K_2NDC	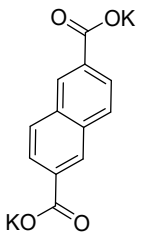	50	116	1M KFSI/EC+DMC (1:1, by vol)	S7
K_4PTC	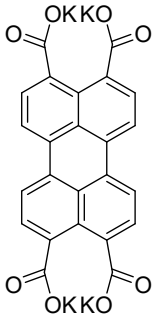	50	97	1M KFSI/EC+DMC (1:1, by vol)	S8
juglone@CNT	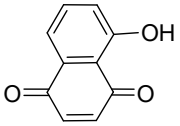	50	241	3 M KFSI/DME	S9
TP-COF HSs		50	197	3 M KFSI/DME	S10

Reference

S1 J. Zou, C. Fu, Y. Zhang, K. Fan, Y. Chen, C. Zhang, G. Zhang, H. Dai, Y. Cao, J. Ma and C. Wang, *Adv. Funct. Mater.*, 2023, **33**, 2303678.

S2 Q. Deng, J. Pei, C. Fan, J. Ma, B. Cao, C. Li, Y. Jin, L. Wang and J. Li, *Nano Energy*, 2017, **33**, 350-355.

S3 S. Li, W. Li, X. Wu, Y. Tian, J. Yue and G. Zhu, *Chem. Sci.*, 2019, **10**, 7695-7701.

S4 C. Li, Q. Deng, H. Tan, H. Wang X, C. Fan, J. Pei, B. Cao, Z. Wang and J. Li, *ACS Appl. Mater. Interfaces*, 2017, **9**, 27414-27420.

S5 C. Li, K.Wang, J. Li and Q. Zhang, *Nanoscale*, 2020, **12**, 7870-7874.

S6 M. Zhang, H. Fei, T. Wang, J. Zhong, L. Wang, H. Luo, S. Tan, Y. Wang, J. Zhu and J. Hu, *Adv. Energy Mater.*, 2019, **9**, 1901663

S7 C. Li, J. Xue, J. Ma and J. Li, *J. Electrochem. Soc.*, 2018, **166**, A5221-A5225.

S8 C. Wang, W. Tang, Z. Yao, B. Cao and C. Fan, *Chem. Commun.*, 2019, **55**, 1801-1804.

S9 Z. Qu, X. Zhang, R. Huang, S. Wu, R. Chen, F. Wu and L. Li, *Nano Lett*., 2022, **22**, 4115–4123.

S10 J. Sun, R. Tian, Y. Man, Y. Fei, X. Zhou, Chin. *Chem. Lett.*, 2023, **34**, 108233